4. P. F. Hopkins *et al.*, *Astrophys. J.* **625**, L71 (2005).
5. B. T. Soifer *et al.*, *Astrophys. J.* **278**, L71 (1984).
6. Data from the HST archive (*34*) at http://archive.stsci.edu/hst/.
7. R. E. A. Fosbury, J. V. Wall, *Mon. Not. R. Astron. Soc.* **189**, 79 (1979).
8. H. A. Thronson, S. Majewski, L. Descartes, M. Hereld, *Astrophys. J.* **364**, 456 (1990).
9. S. A. Eales, E. E. Becklin, K.-W. Hodapp, D. A. Simons, C. G. Wynn-Williams, *Astrophys. J.* **365**, 478 (1990).
10. The Hubble constant H_0 parameterizes how fast the universe is expanding. $\Omega_M \equiv \rho_{matter}/\rho_{critical}$ (where ρ is the mass density) parameterizes the current matter density of the universe, as compared with the critical density that separates open and closed universes. $\Omega_\Lambda \equiv \rho_\Lambda/\rho_{critical}$ parameterizes the current importance of "dark-energy" density in the universe.
11. A distance of 1 pc is approximately equal to 3 light-years.
12. P. Vignati *et al.*, *Astron. Astrophys.* **349**, L57 (1999).
13. S. Komossa *et al.*, *Astrophys. J.* **582**, L15 (2003).
14. R. J. Beswick, A. Pedlar, C. G. Mundell, J. F. Gallimore, *Mon. Not. R. Astron. Soc.* **325**, 151 (2001).
15. J. F. Gallimore, R. Beswick, *Astron. J.* **127**, 239 (2004).
16. E. Egami *et al.*, *Astron. J.* **131**, 1253 (2006).
17. M. Tecza *et al.*, *Astrophys. J.* **537**, 178 (2000).
18. F. Eisenhauer *et al.*, *Astron. Nachr.* **325**, 120 (2004).
19. We measured spatial resolution by taking the FWHM of five star clusters in the nuclear regions. These should be point sources because such clusters are only a few parsecs across, well less than the 30-pc pixel scale of the NIRC2 camera. The average FWHM for these clusters was 0.061 arc sec.
20. A. M. Koekemoer *et al.*, in *Proceedings of the 2002 HST Calibration Workshop*, S. Arribas, A. Koekemoer, B. Whitmore, Eds. (Space Telescope Science Institute, Baltimore, MD, 2002), pp. 341–345.
21. C. E. Max *et al.*, *Astrophys. J.* **621**, 738 (2005) and references therein.
22. P. L. Wizinowich *et al.*, *Proc. SPIE* **4007**, 2 (2000).
23. P. L. Wizinowich *et al.*, *Publ. Astron. Soc. Pac.* **112**, 315 (2000).
24. E. M. Johansson *et al.*, *Proc. SPIE* **4007**, 600 (2000).
25. Details about NIRC2 performance can be found at the instrument Web page, www2.keck.hawaii.edu/inst/nirc2/.
26. Materials and methods are available as supporting material on *Science* Online.
27. L. K. Pollack, C. E. Max, G. Schneider, *Astrophys. J.* **660**, 228 (2007).
28. B. C. Whitmore *et al.*, *Astron. J.* **130**, 2116 (2005) and references therein.
29. S. Komossa, personal communication.
30. L. J. Tacconi *et al.*, *Astrophys. J.* **524**, 732 (1999).
31. J. Binney, S. Tremaine, *Galactic Dynamics* (Princeton Univ. Press, Princeton, NJ, 1987).
32. A. Escala *et al.*, *Astrophys. J.* **630**, 152 (2005).
33. S. Kazantzidis *et al.*, *Astrophys. J.* **623**, L67 (2005).
34. J. Gerssen *et al.*, *Astron. J.* **127**, 75 (2004).
35. *Chandra Proposers' Observatory Guide*, version 8.0, 15 December 2005 (Chandra Science Center, Center for Astrophysics, Harvard University).
36. Chandra relative errors were measured for the "on-axis" bin (0′ to 2′), where it was found that 90% of sources have offsets <0.22″ (*35*).
37. D. Monet *et al.*, *Astron. J.* **125**, 984 (2003).
38. J. Gallimore, personal communication.

39. We thank the staff of the W. M. Keck Observatory, especially D. L. Mignant and the AO team. Data presented here were obtained at the W. M. Keck Observatory, which is operated as a scientific partnership among the California Institute of Technology, the University of California, and NASA. The W. M. Keck Observatory and the Keck II AO system were made possible by generous financial support from the W. M. Keck Foundation. This work was supported in part under the auspices of the U.S. Department of Energy, National Nuclear Security Administration; the University of California, Lawrence Livermore National Laboratory (under contract no. W-7405-Eng-48); and the NSF Science and Technology Center for Adaptive Optics, managed by the University of California at Santa Cruz (under cooperative agreement no. AST-9876783). The authors extend special thanks to those people of Hawaiian ancestry on whose sacred mountain we were privileged to be guests. Without their hospitality, these observations would not have been possible.

Supporting Online Material

www.sciencemag.org/cgi/content/full/1136205/DC1
Materials and Methods
Tables S1 to S3
References

12 October 2006; accepted 27 April 2007
Published online 17 May 2007;
10.1126/science.1136205
Include this information when citing this paper.

Body-Centered Cubic Iron-Nickel Alloy in Earth's Core

L. Dubrovinsky,[1] N. Dubrovinskaia,[2] O. Narygina,[1] I. Kantor,[1] A. Kuznetzov,[3] V. B. Prakapenka,[3] L. Vitos,[4,5,6] B. Johansson,[4,5] A. S. Mikhaylushkin,[6,7] S. I. Simak,[7] I. A. Abrikosov[7]

Cosmochemical, geochemical, and geophysical studies provide evidence that Earth's core contains iron with substantial (5 to 15%) amounts of nickel. The iron-nickel alloy $Fe_{0.9}Ni_{0.1}$ has been studied in situ by means of angle-dispersive x-ray diffraction in internally heated diamond anvil cells (DACs), and its resistance has been measured as a function of pressure and temperature. At pressures above 225 gigapascals and temperatures over 3400 kelvin, $Fe_{0.9}Ni_{0.1}$ adopts a body-centered cubic structure. Our experimental and theoretical results not only support the interpretation of shockwave data on pure iron as showing a solid-solid phase transition above about 200 gigapascals, but also suggest that iron alloys with geochemically reasonable compositions (that is, with substantial nickel, sulfur, or silicon content) adopt the bcc structure in Earth's inner core.

Since the discovery of Earth's core about a century ago, the idea that Fe is the dominant component of the core has gained firm support from geochemical observations, seismic data, the theory of geomagnetism, and high-pressure studies. Strong support for the idea of Fe in the core comes from a reasonably close match between seismologically inferred sound velocities and the density of the core and the measured experimental values for Fe affected by shock and static compression (*1*–*9*). Recent experiments and theoretical calculations proposed the body-centered cubic (bcc) phase as being stable at the conditions of Earth's core (*6*, *7*, *10*, *11*). Cosmochemical data and studies of iron meteorites provide evidence that Earth's core contains substantial (5 to 15%) amounts of Ni (*8*, *9*). Although the study of pure Fe at multimegabar pressures has drawn considerable attention and provided rich experimental data, knowledge about the behavior and properties of Fe-Ni alloys at the conditions of Earth's core is still limited.

Even relatively small amounts of additional components can substantially affect the phase relations and thermophysical properties of Fe alloys (*10*–*13*). At ambient pressure, Fe-Ni alloys with up to 25 atomic % (at %) of Ni have bcc structure, whereas higher Ni contents promote crystallization of the face-centered cubic (fcc)–structured phase. The compression of bcc-structured alloys at ambient temperature results in their transformation to the hexagonal closed-packed (hcp) phase at pressures between 7 and 14 GPa (*10*–*14*) (depending on the composition and conditions of experiments). No further transformations were observed on compression of a $Fe_{0.8}Ni_{0.2}$ alloy up to a pressure of 260 GPa (*1*). The density of $Fe_{0.8}Ni_{0.2}$ when extrapolated to the pressure of Earth's center (360 GPa) is 14.35 g/cm^3, which is close to the density of pure hcp Fe (14.08 g/cm^3) (*1*, *5*). However, the presence of Ni substantially affects phase relations in the Fe-Ni system at high temperatures and pressures (*10*, *14*, *15*). Although the slope of the hcp-fcc phase boundary for pure Fe is 35 to 40 K/GPa (*4*, *5*, *16*), there are indications that the phase boundaries of Fe-Ni alloys with 10 to 30% Ni might have much lower slopes (*13*–*15*) (15 to 25 K/GPa). Therefore, the understanding and interpretation of properties of Earth's core [such as the amount of light elements, seismic anisotropy, fine-scale heterogeneity, and super-rotation (*17*–*20*)] require detailed studies of the Fe-Ni system at high pressures and temperatures.

An Fe-Ni alloy with 9.8(1) at % of Ni was prepared from metallic rods by arc melting of appropriate amounts of Fe (99.999% purity) and Ni (99.999% purity) in an arc furnace in a pure Ar atmosphere. The sample was homogenized in vacuum at 900°C for 150 hours (*12*). In some runs, a

[1]Bayerisches Geoinstitut, Universität Bayreuth, D-95440 Bayreuth, Germany. [2]Mineralogical Institute, Heidelberg University, Im Neuenheimer Feld 236 D-69120 Heidelberg, Germany. [3]Center for Advanced Radiation Sources, University of Chicago, Chicago, IL 60637, USA. [4]Applied Materials Physics, Department of Materials Science and Engineering, Royal Institute of Technology, Brinellvägen 23, SE-100 44, Stockholm, Sweden. [5]Condensed Matter Theory Group, Department of Physics, Uppsala University, Box 530, SE-75121 Uppsala, Sweden. [6]Research Institute for Solid State Physics and Optics, Post Office Box 49, H-1525 Budapest, Hungary. [7]Department of Physics, Chemistry, and Biology, Linköping University, SE-58183 Linköping, Sweden.

Downloaded from www.sciencemag.org on July 26, 2007

natural Fe-7.6%Ni alloy from the Mundrabilla meteorite (*21*) was used as a starting material. The chemical composition and homogeneity of the starting materials and those treated at high-pressure high-temperature conditions were checked by microprobe (SX-50) and scanning electron microscope (LEO-1500) analysis.

In four runs out of dozens of experiments we conducted on Fe-Ni alloys, pressures over 200 GPa were reached (Fig. 1). Three experiments (two on the synthetic $Fe_{0.9}Ni_{0.1}$ alloy and one on the meteorite material) used an internal wire-heating technique (*22*). In these experiments, we used ferropericlase $Mg_{0.87}Fe_{0.13}O$ (which is stable and does not react with the Fe-Ni alloy at high pressure and temperature, at least to the melting point) as a thermal and electrical insulator. A thin layer (about 2 μm thick, 5 μm wide, and 10 μm long) of the probed alloy was attached to Fe electrodes. While slowly increasing the electrical current passing through Fe-Ni foil, we heated the sample and measured the temperature spectroradiometrically (*22*, *23*). Pressure was determined from the Raman signal of a diamond tip (*24*), and thermal pressure was added based on the thermal equation of state (TEoS) of Fe (*5*) (assuming a constant volume of Fe). At pressures above ~230 GPa, we observed reversible discontinuous behavior of resistance as a function of temperature in the temperature interval from 3300 to 3400 K (Fig. 2). The jump in the resistance cannot be associated with melting (because at melting the electrical connection would be broken abruptly) or with chemical reactions [two out of three samples were quenched to ambient conditions and tested with x-ray diffraction and scanning electron microscopy (SEM); no sign of chemical reactions was found]. This suggests that the anomaly in the resistance of the Fe-Ni alloy at pressures above 200 GPa and at high temperatures can be associated with a phase transition. In order to verify the nature of this transition, we performed x-ray diffraction experiments with in situ laser heating.

In experiments at pressures above 150 GPa with in situ x-ray diffraction, a double-sided near-infrared laser heating system at the GeoSoilEnviroCARS research facility at the Advanced Photon Source was used (*15*, *22*, *23*). The size of the laser beam varied from 20 to 30 μm in diameter, with a temperature variation of ±100 K within the beam at temperatures on the order of 3000 K. Heating duration in different experiments was from 10 to 30 min. Temperature was measured by means of multiwavelength spectroradiometry. The high-resolution angle-dispersive x-ray diffraction experiments were performed with 0.3344 Å radiation with a beam size of 5 × 5 μm and a charge-coupled radiation detector. The collected images were integrated in order to obtain conventional diffraction spectra and were processed with the GSAS package (*22*, *23*). In experiments above 100 GPa, we used double-beveled diamonds with culets of 60 or 50 μm installed in a four-pin opposite-plate diamond anvil cell (DAC). Initial holes 40 to 45 μm in diameter were made, and thin (about 3 μm thick) foil of the synthetic $Fe_{0.9}Ni_{0.1}$ alloy was loaded between two layers of single crystals of ferropericlase $Mg_{0.87}Fe_{0.13}O$ in a He atmosphere. Pressure was determined from the equation of state of $Mg_{0.87}Fe_{0.13}O$, which is based on the periclase pressure scale.

On compression to a pressure of ~10 GPa at ambient temperature, the initially bcc-structured $Fe_{0.9}Ni_{0.1}$ alloy started to transform into an hcp phase, similarly to pure Fe or other Fe-Ni alloys with low Ni content (*1*, *5*, *13*–*15*). Upon heating (electrical or laser) the hcp phase transformed (at first partially, and at higher temperatures completely) into the fcc structure (Fig. 1). The fcc phase can easily be temperature-quenched (*15*), and upon compression at ambient temperature it can be observed up to pressures over 200 GPa. However, the highest pressure and temperature at which we observed fcc $Fe_{0.9}Ni_{0.1}$ (together with the hcp phase) in situ were 132 (±10) GPa and 3100 (±100) K (Fig. 1) (*25*). Overall, our data on the hcp-fcc phase boundary of the $Fe_{0.9}Ni_{0.1}$ alloy are in reasonable agreement with the results reported by Lin *et al.* (*10*) (Fig. 1) [especially taking into account the difference in pressure standards used: NaCl by Lin *et al.* (*10*) and periclase in the present work].

When the hcp $Fe_{0.9}Ni_{0.1}$ phase was heated at pressures above 200 GPa, it persisted at least up to 2900 K (Fig. 3A). At a pressure of 225 (±10) GPa and temperature of 3400 (±100) K, we observed a complete transformation of the $Fe_{0.9}Ni_{0.1}$ alloy into the bcc phase (Fig. 3B). This structural transition took place at pressures and temperatures close to the conditions at which the discontinuity

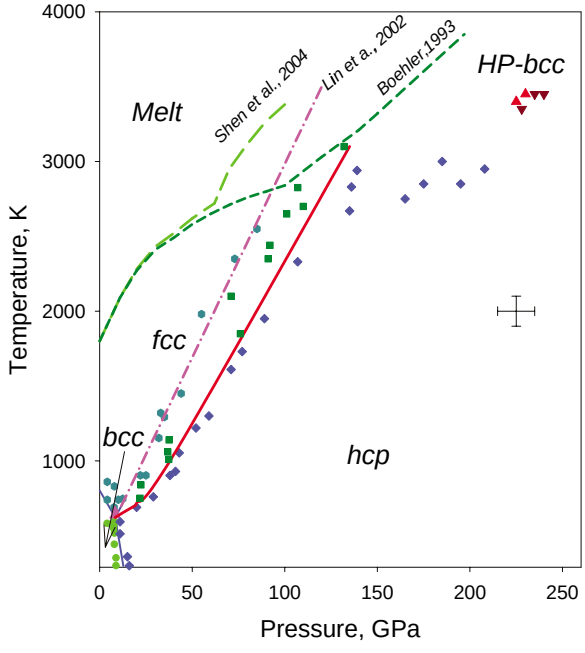

Fig. 1. Phase relations of the $Fe_{0.9}Ni_{0.1}$ alloy at high pressures and temperatures as determined by in situ x-ray diffraction experiments (at pressures below 150 GPa, only points closest to the phase boundaries are shown). Green dots, the low-pressure bcc phase; blue diamonds, the hcp phase; dark cyan hexagons, the fcc phase; dark green squares, the mixture of hcp and fcc phases; magenta triangles, coexistence of bcc, hcp, and fcc phases; red triangles, the high-pressure (HP) bcc phase; dark red inverse triangles, conditions at which discontinuity in electrical resistivity was observed; solid blue lines, phase boundaries between the bcc-hcp and bcc-fcc phases; solid red line, boundary between the hcp phase and the mixture of hcp+fcc phases; dash-dotted purple line, the phase boundary between the hcp phase and the mixture of hcp+fcc phases according to Lin *et al.* (*10*). Melting lines for pure Fe after Shen *et al.* (*16*) and Boehler *et al.* (*3*) are also shown.

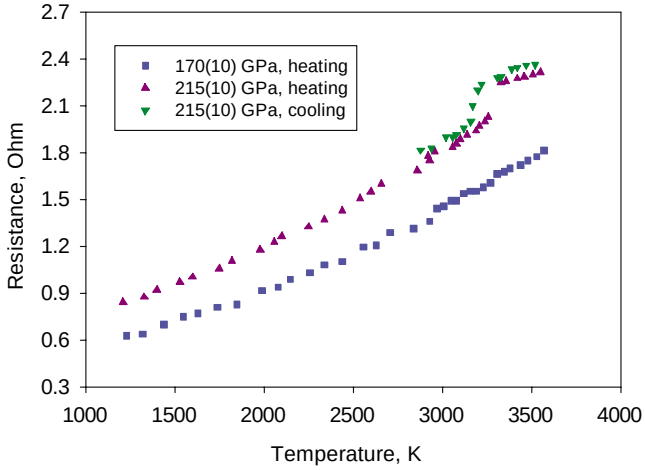

Fig. 2. Dependence of the resistance of the $Fe_{0.9}Ni_{0.1}$ alloy as a function of temperature at two different pressures, given as determined from the Raman signal of a diamond tip (*24*) (at ambient temperature, after heating). At high temperature, thermal pressure should be added. Based on the TEoS of Fe (*5*) and assuming a constant volume of the Fe-Ni alloy at 3400 K, pressure could be estimated as 196 GPa for the lower curve and 240 GPa for the upper curve.

Downloaded from www.sciencemag.org on July 26, 2007

in the resistance has been observed (Figs. 1 and 2). At temperature decrease, the bcc phase completely transformed back to the hcp-structured alloy (Figs. 1 and 3C). On decompression the diamonds failed, but the sample was recovered and its diffraction pattern, as well as the results of examination of the material using SEM, did not reveal any sign of a chemical reaction between the Fe-Ni alloy and ferropericlase or diamond.

The existence of a very-high-pressure bcc phase of pure Fe was proposed long ago (*26*, *27*), but no definitive proof has been obtained so far. We found the hcp-to-bcc phase transition in the $Fe_{0.9}Ni_{0.1}$ alloy at conditions reasonably close to those inferred by Brown and McQueen (*26*) and Brown (*27*) [202 (±2) GPa and 4400 (±300) K] for Fe [the expected (*27*) changes in densities of ~0.7% are also close to those we observed]. This not only supports the interpretation of Brown and McQueen's (*26*) shockwave data as a solid-solid phase transition along the Hugoniout (*6*, *27*) but also suggests that Fe alloys with geochemically reasonable compositions [that is, with substantial Ni, S, or Si content (*7*)] adopt the bcc structure. Indeed, our experiments indicate that the hcp-to-bcc phase transition in $Fe_{0.9}Ni_{0.1}$ alloy occurs at somewhat lower temperature as compared to the conditions at which the transition in pure Fe was observed (*26*, *27*), suggesting that Ni stabilizes the bcc phase in alloys as compared to pure Fe.

In order to understand the effect of Ni on the relative stability of the bcc phase versus the hcp phase in Fe-Ni alloys at high pressure, we carried out first-principles electronic structure calculations (*25*). It turns out that in the (quasi)-harmonic approximation, bcc Fe-Ni alloys are dynamically unstable at high pressure, similar to the case of pure bcc Fe (*7*) (fig. S3). In particular, for $Fe_{0.9}Ni_{0.1}$ we found that the tetragonal elastic constant c' at 300 GPa and 5000 K is negative (–200 GPa) and also that the phonon branches along the [110] and [111] directions are unstable (fig. S3). As a matter of fact, these results are very similar to those obtained for pure bcc Fe (c' = –220 GPa at 300 GPa and 5000 K). The phonon spectra for pure bcc Fe and $Fe_{0.9}Ni_{0.1}$ alloy are also similar (fig. S3). Nevertheless, previous theoretical studies (*6*, *7*) demonstrate that at high temperature, the bcc phase is stabilized by the entropic effects because of anharmonic lattice vibrations. Our calculations clearly show that moderate Ni content (10 to 15%) has a minor effect on the dynamical properties of Fe-Ni alloys, and therefore they must also be stabilized dynamically by the entropic effects, similar to pure Fe. We estimated the impact of Ni on the thermodynamic stability of Fe by calculating (*25*) the energetic effect of the Ni substitution into bcc and hcp Fe at the experimental pressures and at Earth's core pressures. Our first-principles results (fig. S4) show that Ni stabilizes the disordered bcc phase relative to the hcp phase, and the effect of the bcc stabilization clearly increases with increasing Ni concentration and pressure.

The bcc phase of the Fe-Ni alloy experimentally observed in this work (Fig. 1) appears at a pressure of 225 GPa and temperature of 3400 K, which is close to but somewhat lower than the bcc stabilization temperature at this pressure predicted for pure Fe by molecular dynamics simulations (*6*). This is in agreement with the higher stability of bcc Fe-Ni alloys obtained in our study. Most important is that according to our ab initio calculations, the effect of stabilization of the bcc phase of Fe relative to the hcp phase by alloying with Ni increases with pressure and Ni content. Thus, our theoretical results, in combination with earlier studies (*6*, *7*), strongly suggest that the bcc phase of the Fe-Ni

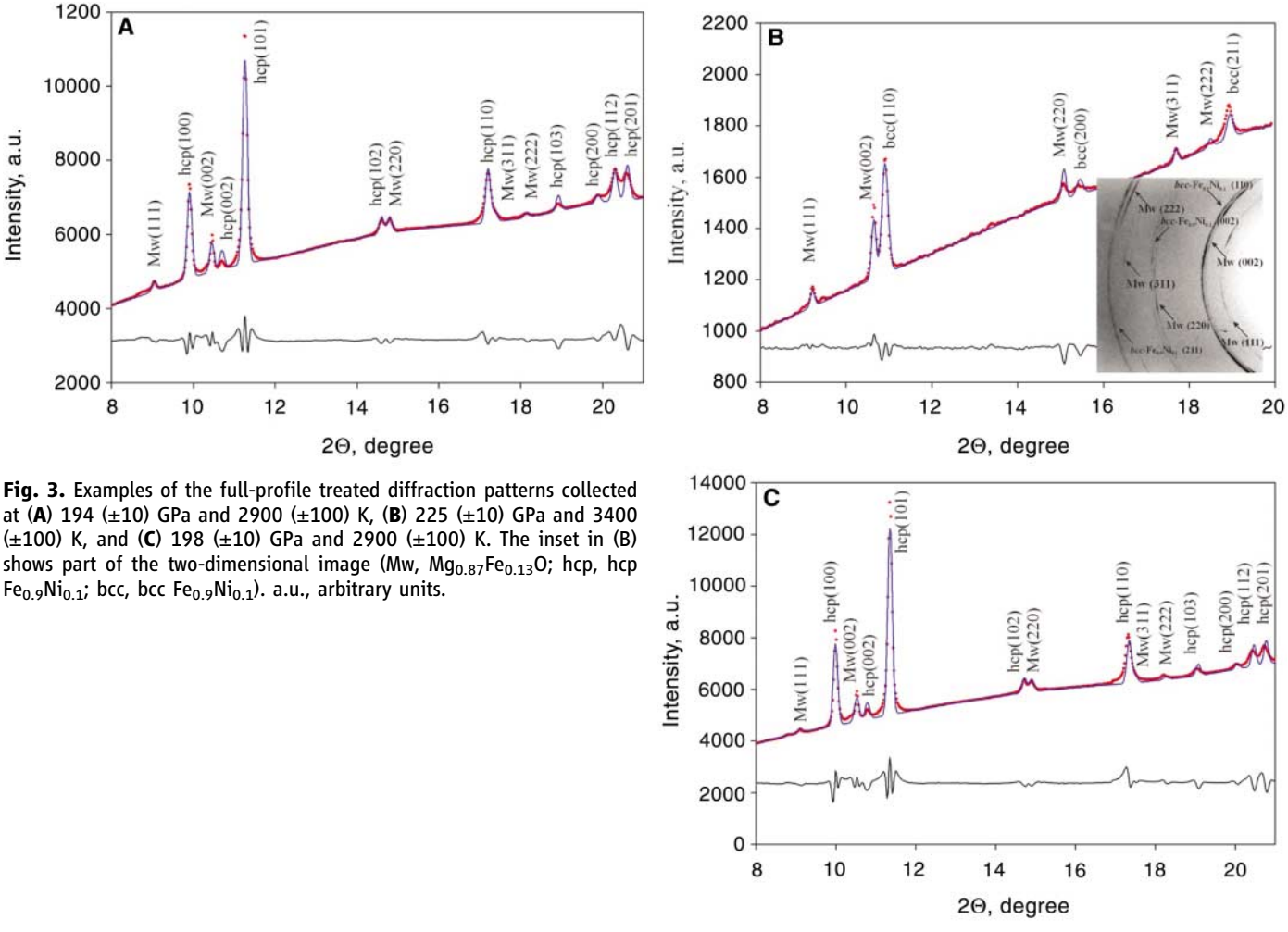

Fig. 3. Examples of the full-profile treated diffraction patterns collected at (**A**) 194 (±10) GPa and 2900 (±100) K, (**B**) 225 (±10) GPa and 3400 (±100) K, and (**C**) 198 (±10) GPa and 2900 (±100) K. The inset in (B) shows part of the two-dimensional image (Mw, $Mg_{0.87}Fe_{0.13}O$; hcp, hcp $Fe_{0.9}Ni_{0.1}$; bcc, bcc $Fe_{0.9}Ni_{0.1}$). a.u., arbitrary units.

Downloaded from www.sciencemag.org on July 26, 2007

alloy with geophysically relevant Ni concentrations (10 to 15%) should be more stable than the hcp phase, not only at the experimental conditions of this work but also at Earth's core conditions.

The experimentally determined lattice parameter of the bcc $Fe_{0.9}Ni_{0.1}$ phase at 225 (±10) GPa and 3400 (±100) K is 2.4884 (±2) Å, which corresponds to a molar volume of 4.64 cm^3/mol and a density of 12.12 g/cm^3. Under the same conditions, hcp Fe has about 2% higher density (*5*). The absolute values of the pressure and changes of density depend on the pressure scale adopted and the hcp Fe TEoS (*25*). If we apply the pressure scale and the hcp Fe TEoS proposed by Dewaele *et al*. (*28*), the pressure in our experiments could be estimated as 195 GPa. This means that in the absence of accurate and self-consistent TEoSs for phases of Fe and Fe-Ni alloys at multimegabar pressure ranges and high temperatures, discussions of the influence of the changes of density produced by the hcp-to-bcc transition of $Fe_{0.9}Ni_{0.1}$ on the density of Earth's inner core are too preliminary. However, it is clear even at this point that bcc $Fe_{0.9}Ni_{0.1}$ is less dense than pure hcp Fe, and the budget of the light elements in the inner core could be reduced because of this phase transition. If conservative estimates are made (*1*, *5*), matching of Earth's inner core density to the preliminary reference Earth model (PREM) does not require any light elements, but at the other extreme [low-temperature (~5200 K) estimates at inner/outer core boundary and pure Fe compressibility described by Dewaele *et al*. (*28*)] the density excess is still about 5%.

The synthesis of bcc $Fe_{0.9}Ni_{0.1}$ at pressures above 230 GPa and temperatures above 3400 K could have implications for understanding the properties and dynamics not only of Earth's solid inner core but of the liquid outer core as well. Changes in the structure of liquids above subsolidus phase boundaries are well known. If changes from "close-packed–like" to "bcc-like" structures occur in molten Fe-Ni alloy at pressures above 200 GPa, this may affect the density and rheology of Earth's outer core as well as the partitioning of light elements between differently structured parts of the molten core.

References and Notes

1. H. K. Mao, Y. Wu, L. C. Chen, J. F. Shu, A. P. Jephcoat, *J. Geophys. Res.* **95,** 21737 (1990).
2. C. S. Yoo, J. Akella, A. J. Campbell, H. K. Mao, R. J. Hemley, *Science* **270**, 1473 (1995).
3. R. Boehler, *Nature* **363**, 534 (1993).
4. D. Andrault, G. Fiquet, M. Kunz, F. Visocekas, D. Häusermann, *Science* **278**, 831 (1997).
5. L. S. Dubrovinsky, S. K. Saxena, F. Tutti, T. Le Bihan, *Phys. Rev. Lett.* **84**, 1720 (2000).
6. A. B. Belonoshko, R. Ahuja, B. Johansson, *Nature* **424**, 1032 (2003).
7. L. Vocadlo *et al.*, *Nature* **424**, 536 (2003).
8. D. Anderson, *Theory of Earth* (Blackwell Scientific, Oxford, 1989).
9. W. F. Bottke, D. Nesvorny, R. E. Grimm, A. Morbidelli, D. P. O'Brien, *Nature* **439**, 821 (2006).
10. J.-F. Lin *et al.*, *Geophys. Res. Lett.* **29**, 109 (2003).
11. J.-F. Lin, D. L. Heinz, A. J. Campbell, J. M. Devine, G. Shen, *Science* **295**, 313 (2002).
12. L. S. Dubrovinsky *et al.*, *Phys. Rev. Lett.* **86**, 4851 (2001).
13. W. L. Mao, A. J. Campbell, D. L. Heinz, G. Shen, *Phys. Earth Planet. Interiors* **155**, 146 (2006).
14. E. Huang, W. Basset, M. S. Weathers, *J. Geophys. Res.* **97**, 4497 (1992).
15. L. Dubrovinsky, N. Dubrovinskaia, in *High-Pressure Crystallography*, *NATO Science Series II, Mathematics, Physics and Chemistry*, A. Katrusiak, P. McMillan, Eds. (Kluwer Academic, Dordrecht, Netherlands, 2004), pp. 393–410.
16. G. Shen, V. B. Prakapenka, M. L. Rivers, S. R. Sutton, *Phys. Res. Lett.* **92**, 185701 (2004).
17. K. C. Creager, *Nature* **356**, 309 (1992).
18. X. D. Song, P. G. Richards, *Nature* **382**, 221 (1996).
19. W. Su, A. M. Dziewonski, R. Jeanloz, *Science* **274**, 1883 (1996).
20. J. E. Vidale, D. A. Dodge, P. S. Earle, *Nature* **405**, 445 (2000).
21. P. Ramdohr, *Fortschr. Mineral.* **53**, 165 (1976).
22. N. Dubrovinskaia *et al.*, *Phys. Rev. Lett.* **95**, 245502 (2005).
23. G. Shen, V. B. Prakapenka, P. J. Eng, M. L. Rives, S. R. Sutton, *J. Synchrotron Radiat.* **12**, 642 (2005).
24. P. Loubeyre, F. Occelli, R. LeToullec, *Nature* **416**, 613 (2002).
25. Materials and methods are available as supporting material on *Science* Online.
26. J. M. Brown, R. G. McQueen, *J. Geophys. Res.* **91**, 7485 (1986).
27. J. M. Brown, *Geophys. Res. Lett.* **28**, 4339 (2001).
28. A. Dewaele *et al.*, *Phys. Rev. Lett.* **97**, 215504 (2006).

29. The authors acknowledge financial support by the European Mineral Sciences Initiative (EuroMinSci) of the European Science Foundation, Deutsche Forschungsgemeinschaft, Swedish Research Council, Carl Tryggers Foundation for Scientific Research, Swedish Foundation for Strategic Research, and Hungarian Scientific Research Fund. Help in sample preparation by A. Audétat and S. Dubravinsky is highly appreciated. Part of this work was performed at GeoSoilEnviroCARS (Sector 13). GeoSoilEnviroCARS is supported by NSF, the U.S. Department of Energy–Geosciences, and the State of Illinois.

Supporting Online Material

www.sciencemag.org/cgi/content/full/316/5833/1880/DC1
Materials and Methods
Figs. S1 to S4
References

5 March 2007; accepted 1 May 2007
10.1126/science.1142105

Reversible Control of Hydrogenation of a Single Molecule

Satoshi Katano,[1] Yousoo Kim,[1]* Masafumi Hori,[1,2] Michael Trenary,[3] Maki Kawai[1,2]*

Low-temperature scanning tunneling microscopy was used to selectively break the N-H bond of a methylaminocarbyne ($CNHCH_3$) molecule on a Pt(111) surface at 4.7 kelvin, leaving the C-H bonds intact, to form an adsorbed methylisocyanide molecule ($CNCH_3$). The methylisocyanide product was identified through comparison of its vibrational spectrum with that of directly adsorbed methylisocyanide as measured with inelastic electron tunneling spectroscopy. The $CNHCH_3$ could be regenerated in situ by exposure to hydrogen at room temperature. The combination of tip-induced dehydrogenation with thermodynamically driven hydrogenation allows a completely reversible chemical cycle to be established at the single-molecule level in this system. By tailoring the pulse conditions, irreversible dissociation entailing cleavage of both the C-H and N-H bonds can also be demonstrated.

The scanning tunneling microscope (STM) can be used to induce a variety of processes of individual molecules, including hopping from one site to another, rotations, conformational changes, bond dissociation, and even bond formation reactions (*1*–*4*). A particularly powerful way to better understand such molecular manipulations with the STM (*5*) is to focus on systems that have already been well characterized by conventional surface science methods and to use inelastic electron tunneling spectroscopy (STM-IETS) (*6*) for chemical identification of reactants and products (*1*, *7*, *8*). The latter method provides a vibrational spectrum of individual molecules, and although several recent examples of its use have been reported, the fundamentals of vibrational excitation with tunneling electrons are still an active area of research (*2*, *3*, *9*). We show here that we can selectively break the N-H bond of a single methylaminocarbyne ($CNHCH_3$, or CNHMe) molecule, without disturbing the C-H bonds, to produce methylisocyanide ($CNCH_3$, or CNMe), and we also can restore the N-H bond at will through an ordinary catalytic hydrogenation reaction. The combination of tip-induced chemistry with surface catalysis thus allows us to produce a repeatable chemical cycle at the single-molecule level.

An earlier study of CNMe on a Pt(111) surface (*10*) was motivated by a desire to determine whether the well-known modes of bonding of CO to Pt(111) (*11*) could be extended to a molecule with the isocyanide (-NC) functionality, which is isoelectronic with CO. In the case of CO, the molecule occupies an on-top site at low surface coverages, but at higher coverages oc-

[1]Surface Chemistry Laboratory, RIKEN, 2-1 Hirosawa, Wako, Saitama 351-0198, Japan. [2]Department of Advanced Materials, University of Tokyo, 5-1-5 Kashiwanoha, Kashiwa, Chiba 277-8651, Japan. [3]Department of Chemistry, University of Illinois at Chicago, 845 West Taylor Street, Chicago, IL 60607–7061, USA.

*To whom correspondence should be addressed. E-mail: maki@riken.jp (M.K.); ykim@riken.jp (Y.K.)

Downloaded from www.sciencemag.org on July 26, 2007